

The Creutz–Taube Complex Revisited: DFT Study of the Infrared Frequencies

Teodora Todorova* and Bernard Delley*

Paul Scherrer Institute, Villigen CH-5232, Switzerland

Received October 1, 2008

The structural parameters, electronic properties, and infrared frequencies of three binuclear ruthenium complexes, $[(\text{NH}_3)_5\text{Ru}(\text{pyrazine})\text{Ru}(\text{NH}_3)_5]^{n+}$, $n = 4-6$, have been investigated with density functional theory. Structural analysis demonstrates that the structure of the mixed-valence 5+, or [II,III], is not an intermediate of the reduced 4+, or [II,II], and the oxidized 6+, or [III,III], compounds. Electronic structure comparison shows that the Ru d_{yz} antibonding orbital is empty when $n = 5$ and 6 and occupied, when $n = 4$. The infrared frequencies have been calculated for a sequence of models with increasingly detailed accounts of counterions, ranging from the free Creutz–Taube 5+ ion, over jellium embedded, CONductor-like Screening MOdel (COSMO), to the experimental structure of the triclinic [II,III](tos) $_5 \cdot 4\text{H}_2\text{O}$ (tos = *p*-toluenesulfonate) crystal. Analysis of the Ru vibrations shows that the spectra for the two symmetry-inequivalent Ru atoms are essentially the same. We find that Ru–Ru modes exist near three well-defined frequencies in the solid: at 145, 285, and 345 cm^{-1} . Similar results are also obtained for the simplified jellium and COSMO models. The spectral properties of these vibrational correlations testify to the existence of two coupled Ru atoms in the same charge state.

1. Introduction

Complexes in which the metal atom is present in more than one oxidation state are of considerable importance in inorganic and bioinorganic chemistry, geology, and molecular electronics.^{1,2} Models of mixed-valence compounds distinguish between two limiting cases of localized and delocalized compounds.³ In the first case, the metal–metal interaction is negligibly weak, and the compound exhibits a two-minima energy surface. The second case corresponds to a single-minimum potential and a very strong interaction between the two metal atoms. Intermediate cases also exist. They are characterized by double-minimum wells with a separating barrier on the order of or smaller than the thermal energy.

The Creutz–Taube ion, $[(\text{NH}_3)_5\text{Ru}(\text{pyrazine})\text{Ru}(\text{NH}_3)_5]^{5+}$ (CT), as a representative of electronically delocalized compounds, has been the subject of a number of interesting experimental^{4–14,35–37,50,56} and theoretical stud-

ies^{15–25,33,34,38–49,52,55} and comprehensive reviews.^{53,54} Originally, the $[(\text{NH}_3)_5\text{Ru}(\text{pyrazine})\text{Ru}(\text{NH}_3)_5]^{5+}$ ion was obtained during efforts to create coordinatively defined and kinetically stable models for an electron transfer.^{4,5} Creutz and Taube synthesized the bis-ruthenium–pentaammine pyrazine complexes in three different oxidation states (4+, 5+, and 6+) and measured the visible and the near-IR spectra.^{4,5} In the mixed-valence complex (5+), a band of 0.79 eV (6400

* Author to whom correspondence should be addressed. E-mail: Teodora.Todorova@psi.ch (T.T.) and bernard.delley@psi.ch (B.D.).

(1) Balzani, V. *Electron transfer in chemistry*; Wiley-VCH: New York, 2001.
 (2) Braun-Sand, S. B.; Wiest, O. *J. Phys. Chem. A* **2003**, *107*, 285.
 (3) Robin, M.; Day, P. *Adv. Inorg. Chem. Radiochem.* **1967**, *10*, 248.
 (4) Creutz, C.; Taube, H. *J. Am. Chem. Soc.* **1969**, *91*, 3988.
 (5) Creutz, C.; Taube, H. *J. Am. Chem. Soc.* **1973**, *95*, 1086.

(6) Citrin, P. H. *J. Am. Chem. Soc.* **1973**, *95*, 6472.
 (7) Beattie, J. K.; Hush, N. S.; Taylor, P. R. *Inorg. Chem.* **1976**, *15*, 993.
 (8) Hush, N. S. *Chem. Phys.* **1975**, *10*, 361.
 (9) Oh, D. H.; Boxer, S. G. *J. Am. Chem. Soc.* **1990**, *112*, 8161.
 (10) Oh, D. H.; Sano, M.; Boxer, S. G. *J. Am. Chem. Soc.* **1991**, *113*, 6880.
 (11) Fürholz, U.; Bürgi, H. B.; Wagner, F. E.; Stebler, A.; Ammeter, J. H.; Krausz, E.; Clark, R. J. H.; Stead, M. J.; Ludi, A. *J. Am. Chem. Soc.* **1984**, *106*, 121.
 (12) Fürholz, U.; Joss, S.; Bürgi, H. B.; Ludi, A. *Inorg. Chem.* **1985**, *24*, 943.
 (13) Best, S. P.; Clark, R. J. H.; McQueen, R. C. S.; Joss, S. *J. Am. Chem. Soc.* **1989**, *111*, 548.
 (14) Delarosa, R.; Chang, P. J.; Salaymeh, F.; Curtis, J. C. *Inorg. Chem.* **1985**, *24*, 4229.
 (15) Demadis, K. D.; Hartshorn, C. M.; Meyer, T. J. *Chem. Rev.* **2001**, *101*, 2655.
 (16) Broo, A.; Larsson, S. *Chem. Phys.* **1992**, *161*, 363.
 (17) Bolvin, H. J. *Phys. Chem. A* **2003**, *107*, 5071.
 (18) Bolvin, H. *ChemPhysChem* **2006**, *7*, 1575.
 (19) Bolvin, H. *Inorg. Chem.* **2007**, *46*, 417.
 (20) Reimers, J. R.; Cai, Z. L.; Hush, N. S. *Chem. Phys.* **2005**, *319*, 39.

cm^{-1}) has been assigned as a metal-to-metal intervalence transition.

X-ray photoelectron spectroscopy (XPS) measurements of the Creutz–Taube ion yield two Ru peaks, seemingly indicating that atoms in two distinct oxidation states are present.⁶ Hush and co-workers propose that the high polarizability of the Creutz–Taube ion could lead to a splitting of the photoionized valence state of the delocalized complex and, therefore, two XPS peaks.^{7,8} Electronic Stark effect studies by Oh et al. show that intervalence adsorption of the Creutz–Taube ion is accompanied by essentially zero charge in the dipole moment and, therefore, zero metal-to-metal charge transfer.^{9,10} These observations are consistent with a description of the complex as fully delocalized in both the ground state and the intervalence excited state. Oh et al. also found that intervalence excitation of $[(\text{NH}_3)_5\text{Ru}(\mu\text{-}4,4'\text{-bipyridine})\text{Ru}(\text{NH}_3)_5]^{5+}$ is accompanied by a large change in dipole moment and, therefore, substantial transfer of charge between metal centers, in line with a valence-localized description. In support of the delocalized form of the Creutz–Taube ion are also the X-ray crystallographic studies that yield identical metal–ligand bond lengths for the two metal centers.^{11,12} Spectroelectrochemical measurements in the IR region show a single NH_3 bend, rather than the pair expected from the simultaneous presence of Ru(II) and Ru(III) centers.¹³ Similar conclusions are supported by Curtis and co-workers, who examined a series of Creutz–Taube ion derivatives (*trans*-ligand $(\text{NH}_3)_4\text{Ru}(\mu\text{-pyrazine})\text{Ru}(\text{NH}_3)_5]^{5+}$ electrochemically.¹⁴ Another point of view is that the Creutz–Taube ion exists in valence-localized form in the ground state but may be delocalized in one or more of the intervalence excited states.¹⁵

Calculations of the $[(\text{NH}_3)_5\text{Ru}(\text{pyrazine})\text{Ru}(\text{NH}_3)_5]^{n+}$ based on wave function theory^{16,17} show that the ground state is better described by a multiconfigurational wave function. Bolvin^{18,19} applied wave-function-based methods to calculate the excited states up to $50\,000\text{ cm}^{-1}$. They form a quasi continuum from $25\,000\text{ cm}^{-1}$. Theoretical bands are assigned to UV–visible spectra, and magnetic circular dichroism bands are assigned by calculating transition moments from first principles for both spectroscopies. *g* factors calculated from first principles and modeled by a model Hamiltonian compare well to experimental values and are the same as in the monomeric species. Reimers and co-workers developed computational procedures by which complete-active-space self-consistent-field and related multireference calculations might be applied to electron-transfer systems whose energetics are controlled by the solvent–solute interaction.^{20,21} As previously pointed out by Bencini et al.,²² Reimers and co-

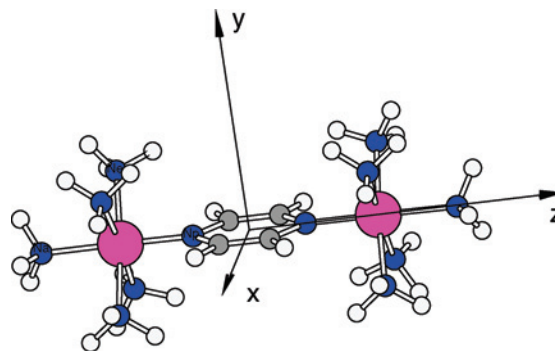


Figure 1. Schematic structure of the Creutz–Taube ion. Purple spheres are Ru atoms; white, hydrogen atoms; blue, nitrogen atoms; and gray, carbon atoms.

workers also found a dependence of the optimized Ru–N bond lengths on the basis set, which contract by $0.09\text{--}0.15\text{ \AA}$ when changing the small LANL2DZ basis set to a moderate-sized SDD one. The effect of the solvation on the Ru–pyrazine separation brings about a 0.18 \AA contraction for the ground state and a massive 0.39 \AA contraction for the excited state. The effective coupling, J , calculated in the gas-phase optimized geometry is 1450 cm^{-1} ²⁰ (a factor of 4 lower than the experimental one),⁵ while DFT calculations of Bencini et al.²² estimated a value of 6800 cm^{-1} at the X-ray geometry. Yokogawa et al.²³ theoretically studied $[(\text{NH}_3)_5\text{M}(\text{lig})\text{M}(\text{NH}_3)_5]^{5+}$, where $\text{M} = \text{Ru}$ or Os and $\text{lig} = \text{pyrazine}$ or $4,4'\text{-bipyridine}$, by a combination of a two-state model²⁴ and a dielectric continuum model. They conclude that the electronic structures of these compounds are very sensitive to the metal, ligand, and solvent. In the gas phase, the structures are delocalized. In aqueous solution, the structures that contain the pyrazine ring are delocalized, while the structures that contain the $4,4'\text{-bipyridine}$ ring are localized.

The present study reports the first complete calculation of the vibrational spectrum for the triclinic $[\text{II,III}](\text{tos})_5 \cdot 4\text{H}_2\text{O}$ by means of density functional theory. Our aim is to reconsider the computationally correct electrostatics by including counterions in the Creutz–Taube ion calculations and comparing the different computational approaches. We test the triclinic $[\text{II,III}](\text{tos})_5 \cdot 4\text{H}_2\text{O}$ crystal in calculating the geometry parameters of the system and compare the results with those for free-ion, jellium, and Conductor-like Screening Model (COSMO) models. Electronic structures for compounds with $n = 4\text{--}6$ by means of the COSMO approach are analyzed.

2. Computational Details

In order to study the Creutz–Taube ion by means of density functional theory calculations, we consider several models. The simplest one consists of two $\text{Ru}(\text{NH}_3)_5$'s bridged by a pyrazine ring, representing a free ion with a charge of $5+$ in the gas phase, as depicted in Figure 1. This free-ion model has been the subject of previous theoretical studies^{22,25} but has not been reported by experiments. More realistic models are those allowing the presence of counterions. A conventional approach to treating charged species in first-principles calculations is using a neutralizing jellium

(21) Tannor, D. J.; Marten, B.; Murphy, R.; Friesner, R. A.; Sitkoff, D.; Nicholls, A.; Ringnalda, M.; Goddard, W. A., III; Honig, B. *J. Am. Chem. Soc.* **1994**, *116*, 11875.

(22) Bencini, A.; Ciofini, I.; Daul, C. A.; Ferretti, A. *J. Am. Chem. Soc.* **1999**, *121*, 11418.

(23) Yokogawa, D.; Sato, H.; Nakao, Y.; Sakaki, S. *Inorg. Chem.* **2007**, *46*, 1966.

(24) Farazdel, A.; Dupuis, M.; Clementi, E.; Aviram, A. *J. Am. Chem. Soc.* **1990**, *112*, 4206.

(25) Hardesty, J.; Goh, S. K.; Marynick, D. S. *THEOCHEM* **2002**, 588, 223.

background charge. The COSMO model^{26–28} involves the construction of a solvent-accessible surface and the solution of electrostatics related to the screening charges located at the solvent-accessible surface. The charge on the solvent-accessible surface is constrained to contain exactly the opposite charge of the solvated compound, including its tail charge, and recently has been generalized for infinite polymer and surface models with periodic boundary conditions.²⁸ Three binuclear complexes, $[(\text{NH}_3)_5\text{Ru}(\text{pyrazine})\text{Ru}(\text{NH}_3)_5]^{5+}$, $n = 4–6$, for the COSMO model have been investigated. In addition to them, we consider a solid-state structure of the triclinic $[\text{II,III}](\text{tos})_5 \cdot 4\text{H}_2\text{O}$ crystal ($\text{tos} = p$ -toluenesulfonate). This crystal structure includes p -toluenesulfonate and H_2O as charge balance species, which practically fill the available interstitial voids, stabilizing the triclinic structure. A partial Hessian method, in which only a sub-block of the Hessian matrix is diagonalized to yield vibrational frequencies for the triclinic $[\text{II,III}](\text{tos})_5 \cdot 4\text{H}_2\text{O}$ crystal, has also been used. It shows that phonon delocalization is not an important effect. The sub-block is selected to contain only the atoms of the $[(\text{NH}_3)_5\text{Ru}(\text{pyrazine})\text{Ru}(\text{NH}_3)_5]$ complex.

The calculations reported in this work are performed by the all-electron density functional theory DMol³ code.^{29,30} A double numerical polarized basis set which includes all occupied atomic orbitals plus a second set of valence orbitals plus polarized d valence orbitals is employed. The Perdew–Burke–Ernzerhof (PBE)³¹ exchange-correlation potential and density functional semicore pseudopotential (DSPP)³² with scalar relativistic corrections to atomic scattering properties are used.

Information on the distribution of molecular levels and their orbital characters is shown graphically in analogy to the partial density of states figures in solid-state studies. The discrete molecular levels are shown as a histogram, and the Mulliken population gives the histogram heights. The orbital type is color-coded. Bars with two colors indicate near degeneracy of orbitals with different symmetries or mixtures.

The vibrational spectrum was calculated in harmonic approximation for all models used here. In the case of solid models, vibrations were calculated at the Γ point of the Brillouin zone only. For a molecular compound, this should be an appropriate approximation. The “ Ru_z ” motions are projected into components along the Ru–Ru line: “stretch” (Q^-), “translation” (Q^+), and components normal to the first two.

3. Results and Discussion

3.1. Structural Analysis. Single-crystal X-ray diffraction experiments¹¹ define two structures, containing the pyrazine-bridged decaammineruthenium $[\text{II,III}]$ ion: (i) in the $[\text{II,III}]\text{Cl}_5 \cdot 5\text{H}_2\text{O}$ compound, the two ruthenium atoms are symmetrically equivalent, and the center of the pyrazine ring coincides with the center of the inversion; (ii) in the $[\text{II,III}](\text{tos})_5 \cdot 4\text{H}_2\text{O}$ compound, the ruthenium atoms are crystallographically inequivalent with a slightly different coordination geometry. The slight structural differences between $[\text{II,III}]\text{Cl}_5 \cdot 5\text{H}_2\text{O}$ and $[\text{II,III}](\text{tos})_5 \cdot 4\text{H}_2\text{O}$ do not show up in the ⁹⁹Ru Mossbauer spectra.¹² Both compounds have

Table 1. Geometrical Parameters of the $[(\text{NH}_3)_5\text{Ru}(\text{pyz})\text{Ru}(\text{NH}_3)_5]^{5+}$ ^a

d[Å, deg]	free ion	COSMO	jellium	solid	experiment
Ru–Ru	7.082	6.807	6.870	6.811	6.781
Ru– N_p	2.109	2.009	2.030	2.027/2.024	1.998/1.972
Ru– N_a	2.144	2.111	2.130	2.129/2.146	2.109/2.126
Ru– N_e	2.146	2.107	2.110	2.141/2.132	2.112/2.112
C– N_p	1.355	1.349	1.350	1.351/1.348	1.376/1.364
CC	1.382	1.369	1.375	1.360/1.365	1.369/1.353
N_pCC	123.1	121.7	122.1	122.0/122.3	121.5/123.2
CN_pC	113.8	116.5	115.8	115.6/115.5	115.1/114.0

^a p denotes pyrazine atoms; a , axial atoms; and e , equatorial atoms. Experimental values are taken from ref 12.



Figure 2. Model structure of the Creutz–Taube ion used for an estimate of the elastic spring constant.

a similar spectrum, which is not midway between $[\text{II,II}]$ and $[\text{III,III}]$. The structural results for the complete electron-transfer series conclusively demonstrate that the mixed-valence ion is not a combination of genuine Ru(II) and Ru(III) moieties. Experiments also consider structures of the Creutz–Taube ion in the liquid phase. However, no stable gas-phase structure has been reported for such a compound.

The geometrical parameters of the Creutz–Taube ion for a free-ion, jellium, COSMO, and triclinic $[\text{II,III}](\text{tos})_5 \cdot 4\text{H}_2\text{O}$ crystal, as obtained with the PBE exchange-correlation potential, are given in Table 1 and are compared with experimental results.¹² We observe a rather large Ru– N_p distance for the free ion, which is reduced when the counterions by the COSMO approach have been applied or a solid $[\text{II,III}](\text{tos})_5 \cdot 4\text{H}_2\text{O}$ crystal has been considered. This behavior is a consequence of the strong electrostatic force when the free ion is highly charged. That pulls the structure apart and elongates the Ru– N_p bonds. To underline this statement, we made an estimate on the elastic spring constant using a simplified model of a Ru–Ru diatomic molecule, shown in Figure 2. The lowest modes involving Ru–Ru stretches are near 100 cm^{-1} . Assuming that the reduced mass also involves the two NH_3 amonia ligands (one on each side, i.e., $\text{NH}_3\text{–Ru–Ru–NH}_3$), a spring constant of $0.04 \text{ Ha}/a_0^2$ has been obtained. Therefore, the elongations in the bonds across the Ru–Ru axis would be 0.4 Å . Refining this model, we include the mass of all five NH_3 ammonia ligands in the estimate (i.e., $5\text{NH}_3\text{–Ru–Ru–}5\text{NH}_3$) and consider again the soft limit frequency of 100 cm^{-1} , as obtained from the IR spectrum. Then, the elongation is reduced to 0.3 Å . That supports the statement that the Ru– N_p bond elongation is a consequence of the $5+$ free-ion model.²² Therefore, the highly charged model of a free ion with no counterions included could not well serve as a reference for further investigations of the Creutz–Taube complex.

Table 2 presents the deviations from the experimental values of the geometrical parameters of $[(\text{NH}_3)_5\text{Ru}(\text{pyz})\text{Ru}(\text{NH}_3)_5]^{5+}$ as obtained in five different studies: The first is the present study with the PBE exchange-correlation functional for cases of a free-ion, jellium, COSMO, and tos crystal. Also shown are the Bencini et al. study²² with PW91 and BP exchange-correlation functionals with and without scalar relativistic corrections, the Reimers et al. study²⁰ with

(26) Klamt, A. *COSMO-RS, from quantum chemistry to fluid phase thermodynamics and drug design*; Elsevier: Amsterdam, 2005.

(27) Andzelm, J.; Kölmel, Ch.; Klamt, A. *J. Chem. Phys.* **1995**, *103*, 9312.

(28) Delley, B. *Mol. Simul.* **2006**, *32*, 117.

(29) Delley, B. *J. Chem. Phys.* **1990**, *92*, 508.

(30) Delley, B. *J. Chem. Phys.* **2000**, *113*, 7756.

(31) Perdew, J. P.; Burke, K.; Ernzerhof, M. *Phys. Rev. Lett.* **1996**, *77*, 3865.

(32) Delley, B. *Phys. Rev. B* **2002**, *66*, 151125.

Table 2. Deviations from the Experimental Values of the Geometrical Parameters of the $[(\text{NH}_3)_5\text{Ru}(\text{pyz})\text{Ru}(\text{NH}_3)_5]^{5+}$ as Obtained in Five Different Studies^a

bond	present study	Bencini et al.	Reimers et al.	Yokogawa et al.	Bolvin
Ru–N _p	+0.111/+0.137 ^a	+0.020/+0.046 ^a	+0.168/+0.194 ^a	+0.004/+0.030	+0.002/+0.028
	+0.032/+0.058 ^b	+0.028/+0.054 ^b	+0.259/+0.285 ^b		
	+0.011/+0.037 ^c	–0.011/+0.015 ^c	+0.081/+0.107 ^c		
	+0.029/+0.052 ^d	+0.006/+0.026 ^d			
Ru–N _a	+0.035/+0.018 ^a	+0.003/–0.014 ^a	+0.076/+0.059 ^a	+0.026/+0.009	+0.025/+0.008
	+0.021/+0.004 ^b	+0.007/–0.010 ^b	+0.071/+0.054 ^b		
	+0.002/–0.015 ^c	+0.000/–0.015 ^c	+0.045/+0.028 ^c		
	+0.020/+0.020 ^d	–0.001/–0.018 ^d			
Ru–N _e	+0.034/+0.034 ^a	+0.004/+0.004 ^a	+0.080/+0.080 ^a	–0.002/–0.002	–0.002/–0.002
	–0.002/–0.002 ^b	+0.008/+0.008 ^b	+0.092/+0.092 ^b		
	–0.005/–0.005 ^c	+0.007/+0.007 ^c	+0.056/+0.056 ^c		
	+0.029/+0.020 ^d	–0.003/–0.003 ^d			

^a Present study: PBE exchange–correlation functional, (a) free ion, (b) jellium, (c) COSMO, and (d) tos crystal. Bencini et al.:²² (a) PW91, nonrelativistic; (b) BP nonrelativistic; (c) PW91 relativistic; (d) BP relativistic. Reimers et al.:²⁰ (a) SDD basis set, gas phase; (b) LANL2DZ basis set, gas phase; (c) LANL2DZ basis set, ESP SCRF solvation model.²¹ Yokogawa et al.:²³ combination of a two-state model²⁴ and dielectric continuum model. Bolvin:¹⁹ CASSCF (complete active space self-consistent field)/CASPT2 (perturbation theory at the second order).

SDD and LANL2DZ basis sets in the gas phase and ESP SCRF solvation model,²¹ the Yokogawa et al. study²³ using a combination of a two-state model²⁴ and a dielectric continuum model, and the Bolvin¹⁹ complete active space self-consistent field/perturbation theory at the second order (CASSCF/CASPT2) study. Results show that DFT methods are as good as multireference wave-function-based methods in describing the ground-state properties of the Creutz–Taube ion. The smallest deviation obtained by both, the DFT and the multireference wave-function-based methods, is –0.002 Å for the Ru–N_e bond, where the Yokogawa model, the Bolvin model, and the jellium model of the present study give the same result. The biggest deviation is in the Ru–N_p bond in the gas-phase calculations, where the present study overestimates the bond by +0.137 Å, while Reimers et al. found a value of +0.285 Å with a moderate basis set. While the description of the environment by a solvation model strongly improves the quality of the geometry optimization, it has no effect on the nature of the ground and excited states.²³ On the contrary, ab initio multiconfiguration self-consistent field and intermediate neglect of differential overlap methods combined with Monte Carlo simulations suggest that the effect of the solvent on the electronic structure of the solute is to reduce the magnitude of the change in dipole moment upon metal-to-ligand charge-transfer absorption.³³ DFT calculations are well-suited for the determination of energies and geometries of the ground state of specific spin and orbital symmetries. The use of wave-function-based theory, however, permits the full description of all of the excited states, most of them being by far not monodeterminal. Bond length changes upon changing the oxidation state of the metal are not fully reproduced.³⁴ A comparative DFT-MP2 study of the Creutz–Taube ion points to the enhanced ionic character of the Ru–N bond in the MP2 calculations.²⁵ The Ru–N bond is overestimated by 0.04–0.18 Å in the DFT and by 0.01–0.05 Å in the MP2 calculations.

Table 3 shows a comparison of structural parameters, for the 4+, 5+, and 6+ compounds, as obtained by the COSMO model. The [II,III] structure, representing the 5+ compound, is not between the completely oxidized [III,III] representing the 6+ compound and the completely reduced [II,II]

Table 3. Geometrical Parameters of the COSMO $[(\text{NH}_3)_5\text{Ru}(\text{pyz})\text{Ru}(\text{NH}_3)_5]^{n+}$ ^a

d[Å]	n = 4	n = 5	n = 6
Ru–N _p	2.066(2.013)	2.009(1.991)	2.074(2.115)
Ru–N _a	2.197(2.149)	2.111(2.123)	2.188(2.089)
Ru–N _e	2.176(2.132)	2.107(2.112)	2.175(2.101)
C–N _p	1.362(1.353)	1.349(1.362)	1.362(1.341)
CC	1.381(1.363)	1.369(1.361)	1.382(1.382)

^a Experimental values in parentheses are taken from ref 12.

representing the 4+ compound. For the [II,II] and [II,III], lengthening of the C–N and contraction of the C–C bonds are observed, as in the experiments (values are given in parentheses), which is an indication of electron transfer from the Ru to the lowest unoccupied molecular orbital of the pyrazine ring. The C–N and the C–C distances of the [III,III] structure, representing the 6+ compound, are very close to that of the free pyrazine; no contraction of the C–C bond is observed. Therefore, there is no indication of backdonation for the 6+ compound. Results of others propose that $(\text{NH}_3)_5\text{Ru}^{\text{II}}(\text{pyrazine-CH}_3)^{3+}$ and $(\text{NH}_3)_5\text{Ru}^{\text{III}}(\text{pyrazine-CH}_3)^{4+}$ display Ru–N_p bond lengths that differ by 0.13 Å.³⁵

3.2. Electronic Structure. In both experimentally determined structures, the ruthenium centers clearly “communicate” through the bridging ligand. It has been proposed³⁶ that one electron in the 4d⁶ subshell is either delocalized between the Ru atoms or alternatively trapped at one Ru center: in the former case, the ion will have a symmetric delocalized electronic ground state with a metal average valence of +2.5, while in the latter case, the system would have two states with equal energy, which leads to trapped metal valences, RuII–RuIII or RuIII–RuII, and the electron would transfer between two potential wells with an equal

(33) Zeng, J.; Hush, N. S.; Reimers, J. R. *J. Am. Chem. Soc.* **1996**, *118*, 2059.

(34) Broo, A.; Lincoln, P. *Inorg. Chem.* **1997**, *36*, 2544.

(35) Wishart, J. F.; Bino, A.; Taube, H. *Inorg. Chem.* **1986**, *25*, 3318.

(36) Creutz, C. *Prog. Inorg. Chem.* **1983**, *30*, 1.

(37) Streckas, T. C.; Spiro, T. G. *Inorg. Chem.* **1976**, *15*, 974.

(38) Sizova, O. V.; Baranovskii, V. I.; Panin, A. I.; Ivanova, N. V. *J. Struct. Chem.* **1999**, *39*, 471.

(39) Leshchev, D. V.; Baranovskii, V. I.; Sizova, O. V.; Panin, A. I. *J. Struct. Chem.* **1999**, *40*, 493.

(40) Zhang, L. T.; Ko, J.; Ondrechen, M. J. *J. Am. Chem. Soc.* **1987**, *109*, 1666.

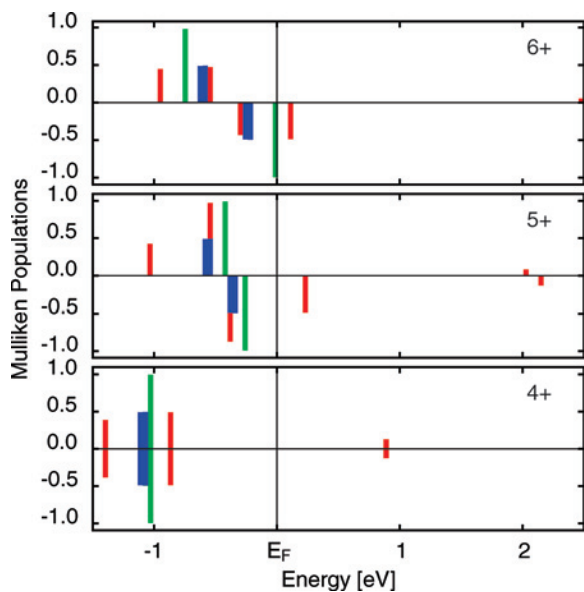


Figure 3. The levels from the COSMO solvated model as a density of states histogram for 4⁺, 5⁺, and 6⁺ compounds: d_{yz} in red, $d_{x^2-y^2}$ in green, and d_{xz} in blue.

depth in an intramolecular electron-transfer process. The two Ru $4d_{yz}$ orbitals strongly mix with one π^* orbital on the pyrazine bridge, which is an indication for a delocalized or valence-averaged ground state. Macroscopic evidence of the π -back-donation is the shortening of the C–C bond and the lengthening of the C– N_p bond computed when passing from the free ligand to the ligand inside the complex. Arguments of Streckas and Spiro,³⁷ who proposed a trapped valency for the ground state, were based on the measured [II,III] spectrum, which is closer to that of the [II,II] but, in addition to it, possesses a line at 1070 cm^{-1} , which is a characteristic line for the Ru(III) state.

Figure 3 shows a combined picture of orbital levels and orbital characters by Mulliken population analysis of the three binuclear complexes, $[(\text{NH}_3)_5\text{Ru}(\text{pyrazine})\text{Ru}(\text{NH}_3)_5]^{n+}$, $n = 4-6$, as obtained with the COSMO approach. A very similar density of states picture is also obtained for the crystalline compound, where the level picture is drowned in the multitude of crystalline orbitals with d admixtures. The populations are nearly 0.5, as the orbitals are bonding and antibonding Ru d orbitals with little other admixtures. The histogram picture is simply related to the customary level picture by a mirror operation on the 45° axis. Each histogram corresponds to a level; majority spin is shown positive, and minority spin is shown as negative. The colors give information about the d population on the Ru_1 atom.

In the COSMO 4⁺ case, the electronic structure has a closed shell. Removing one electron from the compound, depopulates an orbital of the d_{yz} type, and spin polarization occurs (the 5⁺ case). The d_{yz} orbital is depopulated, and the antibonding character of the Ru– N_p bond is decreased. This is confirmed by the shorter Ru– N_p distances. The Ru d_{yz} states with spin-up and spin-down polarization shift to higher energy. So do the $d_{x^2-y^2}$ and d_{xz} states. While in the 4⁺ state, the d_{yz} energy levels are occupied, in the 5⁺ case, the spin-down d_{yz} state is empty. When another electron is removed from the 5⁺ compound and the 6⁺ compound is achieved,

Table 4. Mulliken Atomic Charges on the Atoms of the $[(\text{NH}_3)_5\text{Ru}(\text{pyz})\text{Ru}(\text{NH}_3)_5]^{5+}$ Compound^a

atom	free ion	COSMO	jellium	solid
Ru	1.952	0.721	0.898	0.603
N_p	−0.731	−0.282	−0.306	−0.297
N_a	−1.658	−1.041	−0.981	−1.030
C_p	−0.330/−0.347	−0.102/−0.108	−0.036/−0.040	−0.086/−0.098
H_p	0.427/0.396	0.336/0.340	0.307/0.308	0.388/0.422
H_a	0.621/0.594	0.431/0.463	0.414/0.399	0.385/0.429

^a p denotes pyrazine atoms; a , axial atoms.

a charge redistribution occurs. The spin-up states move slightly down in energy; the spin-down states below the top of the valence band move slightly up in energy. The d_{yz} antibonding state is above the Fermi level and is depopulated. The nonbonding $d_{x^2-y^2}$ state is at the top of the valence band. Withdrawing electrons from the upper energy levels has an indirect effect on the Ru– N_p bonding: the charge redistribution increases the electrostatic repulsion and weakens the bonds. This explains the longer bonds for $n = 6$, compared to $n = 4$ and 5. These results are in line with the results from the ab initio and semiempirical studies of Broo and Larsson.¹⁶

The Mulliken population analysis is presented in Table 4. When counterions are included in the calculations, the charge is more delocalized within the compound than without. The jellium model distributes the charges of the counterions uniformly around the compound. The COSMO model and the solid calculations show similar results. Both leave a lesser amount of charge on the carbon atoms from the pyrazine ring compared to the free-ion model. Mulliken population analysis, for the highly charged free ion, gives values of +1.925 on the Ru atoms and −0.731 on the N atoms of the pyrazine ring which is more than twice the value for the solid, COSMO and jellium models, which involve external countercharges. The N atoms of the terminal ligands NH_3 have charges of −1.658 for the free ion and around −1.0 for the solid, COSMO, and jellium models. A negative charge of −0.330/−0.347 is concentrated on the C atoms belonging to the pyrazine ring and more than three times less for the rest of the cases. The H atoms of the pyrazine ring have positive charges of +0.396/+0.427, while those of the terminal groups have charges of +0.594/+0.621. Here, the four cases are in agreement. The terminal N_a 's are more negative compared to those of the pyrazine ring N_p 's, while the H_a atoms are more positive than that of the pyrazine ring H_p , except in the solid-state calculations, where there is almost no difference.

A quantum-chemical study of the magnetic properties and electronic structure of the Creutz–Taube ion suggests that the electronic structure of this ion is localized,^{38,39} in contrast to the studies of Ondrechen and co-workers, which show that the unpaired spin is shared equally by the two metal ions.^{40–46} Electronic structure calculations by means of the Hartree–Fock–Slater discrete variational method suggest

(41) Ondrechen, M. J.; Ko, J.; Zhang, L. T. *J. Am. Chem. Soc.* **1987**, *109*, 1672.

(42) Ondrechen, M. J.; Ellis, D. E.; Ratner, M. A. *Chem. Phys. Lett.* **1984**, *109*, 50.

(43) Ondrechen, M. J.; Ko, J.; Root, L. J. *J. Phys. Chem.* **1984**, *88*, 5919.

(44) Ko, J.; Ondrechen, M. J. *Chem. Phys. Lett.* **1984**, *112*, 507.

that there is a strong mixing of the two Ru $4d_{yz}$ orbitals with one π^* orbital of the pyrazine bridging ligand.⁴⁰ They form bonding, nonbonding, and antibonding configurations. The intervalence transfer band is at 6400 cm^{-1} and is described as a bonding-to-nonbonding transition. A delocalized mixed-valence system is also suggested by the vibronic coupling model calculations of Piepho et al.^{48,49} Their calculations^{48,49} indicate that, in addition to the π^* orbital, the π orbitals of the pyrazine bridging ligand also likely participate—a point also emphasized by Chou and Creutz.⁵⁰ Ab initio and semiempirical studies of electron transfer and spectra of binuclear complexes with organic bridges confirm the accepted interpretation that there is a strong yz coupling via the pyrazine π orbitals for $[(\text{NH}_3)_5\text{Ru}(\text{pyrazine})\text{Ru}(\text{NH}_3)_5]^{n+}$, when $n = 5$, and a very weak antiferromagnetic coupling between the metal ions, when $n = 6$.¹⁶

DFT calculations favor a delocalized mixed-valence compound. This turns out to be structurally consistent with the experimental findings for the crystalline compound¹¹ where agreement of our calculated structure around the Ru atoms is at the 0.02 \AA level of accuracy for $n = 5+$, Table 3.

The lowest dipole-allowed transition is for minority spin from bonding d_{yz} to the antibonding d_{yz} orbital, which is at about 5000 cm^{-1} for the $5+$ ion. This is lower than the observed IR transition at 6400 cm^{-1} . Part of that error probably has to be ascribed to the localization–delocalization errors currently unavoidable with DFT, which leads to the well-known underestimation in band gap predictions. This error can also be viewed as a consequence of the self-interaction errors, which are particularly prominent when systems dissociate with fractional charges on the separated subunits.⁵¹ In this context, it may be remarked that the high overall charge of the Creutz–Taube cation does not lead to particular problems. In the free ion, the obvious problem can be dubbed Coulomb swelling. This disappears for the jellium counter charge model and the COSMO solvation model, where the charge is forced to be localized on the ion. The full crystal system would, in principle, allow fractional charge partitioning between the cation and anion. However, no fractional charge problem becomes apparent, and the cation levels are consistent with the simpler models where localization of the $5+$ charge is forced by construction.

The DFT calculations yield adiabatic states within the Born–Oppenheimer approximation. The energy scale for the splitting of the electronic state implies an electronic matrix

element of $0.3\text{--}0.5\text{ eV}$, coupling the diabatic states underlying the d_{yz} bonding–antibonding transition. Matrix elements of vibronic coupling are about 1 order of magnitude smaller. A small model calculation including vibronic coupling as a perturbation to our adiabatic states suggests that the lowest IR excitation shifts to slightly larger energy. The vibronically coupled ground state has a small admixture of the antibonding d_{yz} orbital to the bonding one. This is a small step toward localization of the d_{yz} minority spin electron on one Ru atom. A more complete evaluation of vibronic matrix elements and more complete study of the vibronically coupled Hamiltonian must be postponed to a later study.

3.3. Infrared Frequencies. The Creutz–Taube complex was first isolated in the solid state as a tosylate salt. The IR spectra obtained are difficult to interpret due to the superposition of bands, because of the organic anion. To eliminate this problem, the bromide salt of a Creutz–Taube $5+$ ion together with the bromide salt of the corresponding Ru(III)–Ru(III) $6+$ and Ru(II)–Ru(II) $4+$ complexes were prepared. It was found that IR bands attributable to the $5+$ complex are not a superposition of the $4+$ and $6+$ complexes.⁷ Where the bands of $5+$ were measurable, a single band was found at a position intermediate between the corresponding bands of the $4+$ and $6+$ complexes. A NH_3 frequency of 800 cm^{-1} was found for the $5+$ ion: the corresponding frequencies for the $4+$ and $6+$ complexes were 750 and 800 cm^{-1} , respectively. A mode with a frequency of 449 cm^{-1} is attributed to the Ru– NH_3 stretch for the $5+$ ion, while the corresponding frequencies for the $4+$ and $6+$ complexes are 438 and 461 cm^{-1} , respectively. Creutz and Taube also measured some IR bands of salts of the $5+$ ion.⁵ They noted that bands obtained for the $5+$ ion are “rather intermediate” between those of the $4+$ and $6+$ complexes and found no evidence of superposition of the $4+$ and $6+$ bands in the $5+$ spectra. Two independent DFT studies performed a line search exploration of the adiabatic energy surface, involving two line search directions each.^{22,52} Here, we calculate the complete set of 156 normal modes for our molecular models. In the case of the crystalline model, we calculate the full set of 312 Γ -point modes for the partial Hessian of the two embedded ions in the crystal (Figure 4b). We also calculate the full set of 924 Γ -point modes, which includes the counterions of the crystal model (Figure 4a). In order to extract spectral properties of modes involving the metal atoms, a mode projection method is used, which is sketched in the Appendix.

Further, we perform an analysis of the Ru local vibrations and obtain spectral plots, which cover a vibration range from 0 to 550 cm^{-1} . The partial densities for the vibrations of the two crystallographically inequivalent Ru atoms are essentially the same. The main property, which shows that the two Ru atoms are in the same charge state, is the distinct Ru–Ru stretch frequencies (red–red–green sequence). We find that Ru–Ru stretch type exists near two well-defined frequencies in the solid: at 145 and 285 cm^{-1} (Figure 4, Q^- , in red). A Ru–Ru translation along the bond exists at a clearly different frequency of 345 cm^{-1} (Figure 4, Q^+ , in green). Similar results are obtained for the simplified jellium and COSMO

(45) Root, L. J.; Ondrechen, M. J. *J. Chem. Phys. Lett.* **1982**, *93*, 421.

(46) Ferretti, A.; Lami, A.; Ondrechen, M. J.; Villani, G. *J. Phys. Chem.* **1995**, *99*, 10484.

(47) Lu, H.; Petrov, V.; Hupp, J. T. *J. Chem. Phys. Lett.* **1995**, *235*, 521.

(48) Piepho, S. B.; Krausz, E. R.; Schatz, P. N. *J. Am. Chem. Soc.* **1978**, *100*, 2996.

(49) Piepho, S. B. *J. Am. Chem. Soc.* **1990**, *112*, 4197.

(50) Creutz, C.; Chou, M. H. *Inorg. Chem.* **1987**, *26*, 2995.

(51) Cohen, A. J.; Mori-Sánchez, P.; Yang, W. *Science* **2008**, *321*, 792.

(52) Chen, Z.; Bian, J.; Zhang, L.; Li, S. *J. Chem. Phys.* **1999**, *111*, 10926.

(53) Crutchley, R. J. *Adv. Inorg. Chem.* **1994**, *41*, 273.

(54) Hupp, J. T. *Comp. Coord. Chem II* **2004**, *2*, 709.

(55) Reimers, J. R.; Wallace, B. B.; Hush, N. S. *Philos. Trans. R. Soc. London, Ser. A* **2008**, *366*, 15.

(56) Petrov, V.; Hupp, J. T.; Mottley, C.; Mann, L. C. *J. Am. Chem. Soc.* **1994**, *116*, 2171.

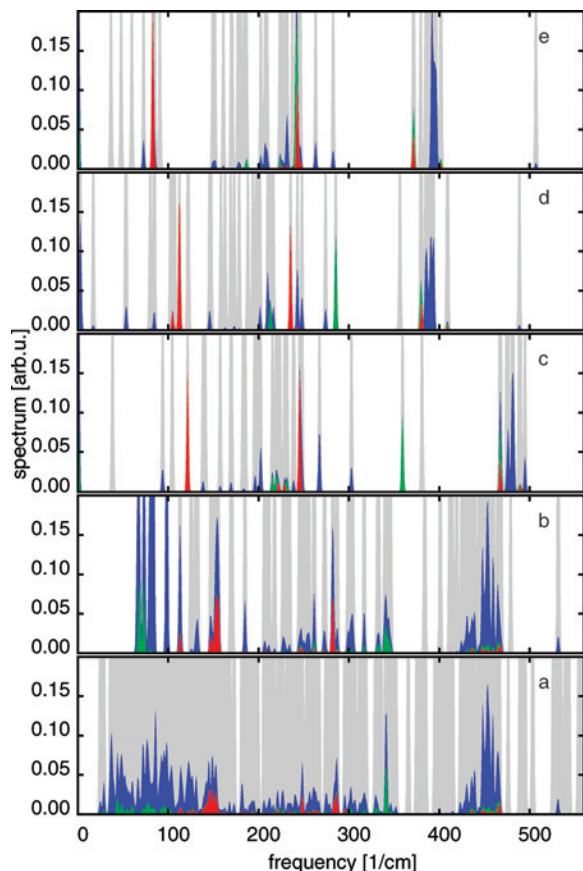


Figure 4. Infrared spectrum of the triclinic [II,III](tos)₅·4H₂O crystal (a), the spectrum obtained by a partial Hessian method (b), the COSMO (c), jellium approaches (d), and the free ion model (e). Ru–Ru symmetric stretches are given in red (Q[−]). Ru–Ru translation along the bond is given in green (Q⁺), and in blue are the complementary, (Q⁺) and (Q[−]), Ru–Ru stretches for the 5⁺ compound. Remaining total spectral intensity is given in gray.

models. We also consider a calculation based on the partial Hessian for the real crystal, which confirms the findings for the positions of Q⁺ and Q[−] in the Ru IR spectrum (Figure 4). The spectral properties of these vibrational correlations testify to the existence of two coupled Ru atoms in the same charge state and point to the delocalized nature of the Creutz–Taube ion. We compare the three spectra of the 4⁺, 5⁺, and 6⁺ complexes, as obtained with the COSMO approach (Figure 5). The figures show that the spectrum of [II,III] is not in between those of [II,II] and [III,III]. The symmetric line at around 100 cm^{−1} is shifted to higher frequencies for the 5⁺, in contrast to the 4⁺ and 6⁺ compounds. The other symmetric line at around 237 cm^{−1} is almost identical for the three types of compounds. The antisymmetric line at 290 cm^{−1} for the 4⁺ compound is shifted to 350 cm^{−1} for the 5⁺ and 310 cm^{−1} for the 6⁺ compound. Complementary (Q⁺ and Q[−] vibrations given in blue) are found around 400 cm^{−1}: below 400 cm^{−1} for the 4⁺, at 475 cm^{−1} for the 5⁺, and below 400 cm^{−1} for the 6⁺. Two symmetry-related and coupled Ru–NH₃ stretching vibrations have also been found by others at 400 cm^{−1} and at 440 cm^{−1} for the localized Ru²⁺(NH₃)₅ and for the localized Ru³⁺(NH₃)₅ units, respectively.⁵⁵

The need to include the solute–solvent interactions for more accurate understanding has been highlighted re-

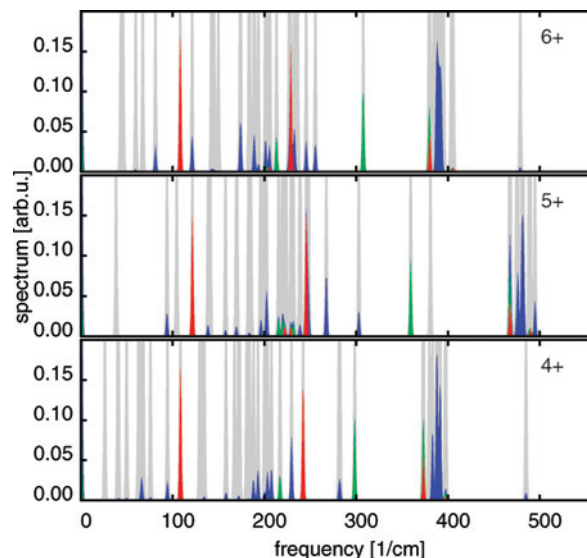


Figure 5. Infrared spectra calculated with the COSMO approach. Ru–Ru symmetric stretches are given in red (Q[−]). Ru–Ru translations along the bond are given in green (Q⁺), and in blue are the complementary, (Q⁺) and (Q[−]), Ru–Ru stretch modes for the 4⁺, 5⁺, and 6⁺ compounds. Remaining total spectral intensity is given in gray.

cently.^{15,55} The present study involves a hierarchy of increasingly detailed treatment of such interactions. While the free molecular ion neglects the solvent environment altogether, the jellium already includes a blurred distribution of counter charge. The COSMO model wraps the Creutz–Taube ion with countercharges mimicking a high dielectric solvent such as water. The partial Hessian crystal model includes the real counterions present in the crystal in a static way. The full crystal model furthermore allows delocalization of vibrational modes onto the counterions. Figure 4 shows the increasing complexity of the vibrational spectrum (e → a).

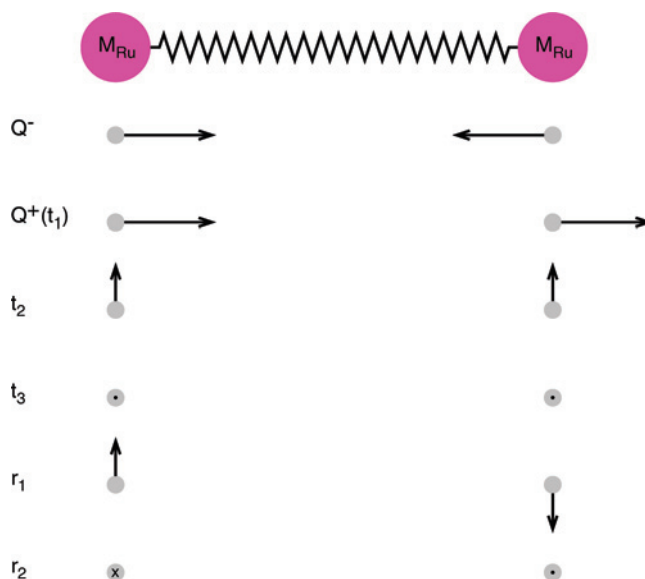
The four spectra obtained with the triclinic [II,III](tos)₅·4H₂O crystal, partial Hessian method, and the jellium and the COSMO models and for the 4⁺, 5⁺, and 6⁺ compounds show that the pattern in the frequency distribution is symmetric stretch–symmetric stretch–antisymmetric stretch (red–red–green). In the free-ion model, the ruthenium Q⁺ and Q[−] vibrations (at 237 cm^{−1} and 380 cm^{−1}) are practically degenerate (Figure 4e). This is evidence for the weak Ru–Ru coupling remaining with the 5⁺ complex in a vacuum. Figure 2 shows the simplified one-dimensional model of the Creutz–Taube complex. In a limit of a very strong coupling between the Ru (purple sphere) and the ligand (green sphere) and negligible coupling between the two Ru atoms, one would have two stretching frequencies and two modes with frequencies of zero. In another limit, where the coupling between the ligand and the Ru is negligible, compared to that of the Ru–Ru, one would have a symmetric stretch and three frequencies of zero. In the case of a system such as ligand–Ru–Ru–ligand as shown in Figure 2, one would expect a symmetric–antisymmetric–symmetric stretch (red–green–red). However, this is not the case according to the IR spectrum we obtained using four methods and three different systems, where the pattern in the frequency distributions shows symmetric stretch–symmetric stretch–

Table 5. Infrared Frequencies as Obtained by Experimental (RR, Resonance Raman; TD, Time-Dependent; IRV, Infrared Vibrational) and Theoretical Methods and Reported in the Literature

reference	method	Ru–N _{pyrazine}	Ru–NH ₃
56	RR spectroscopy	326	334
37	R spectroscopy	328	n/a
47	RR and TD scattering	324	262
7	IRV spectroscopy	n/a	449
52	DFT (ADF)	430	430
22	DFT (ADF, DiNa)	359; 139	n/a
present study	DFT (DMol ³)	145; 285; 345	450

antisymmetric stretch (red–red–green). A calculation of infrared frequencies of a linear chain that contains five bodies shows a spectrum pattern of an antisymmetric–symmetric–antisymmetric stretch. A six-body linear chain, however, reveals the pattern we obtain for the Creutz–Taube complex, that is, symmetric stretch–symmetric stretch–antisymmetric stretch (red–red–green). It is a part of the complete spectrum obtained for the six-body chain model, containing three red and two green lines, which identify the three symmetric and the two antisymmetric stretches. Simplifying the mechanical model of the linear chain from a six-body to a four-body model makes the lines in the spectrum disappear, and that causes a loss of physically valuable information. Representing the pyrazine ring as a single body (five-body linear chain model) misses the important N–N vibrations and shows another pattern in the frequency distribution. Therefore, the complete model structure, which explains the infrared spectrum of the Creutz–Taube complex, consists of six bodies: ligand–Ru–N–N–Ru–ligand. This finding suggests that the N–N vibrations of the pyrazine ring cannot be neglected and implies a strong pyrazine effect on the Ru–Ru stretches in the compound. The importance of the Ru–pyrazine–Ru coupling has been recognized using resonance Raman studies in the extended near-infrared region.⁵⁶ These studies underline the role of a three-site mixing mechanism on the valence delocalization in the Creutz–Taube ion. They also propose a strong coupling of pyrazine bridge motions to the intervalence transition. Coupling to the symmetric bridge mode suggests a direct involvement of pyrazine orbitals in the intervalence excitation process. It also implies pyrazine participation in the delocalization process. Therefore, the three-site mixing (Ru–pyrazine–Ru) rather than conventional two-site coupling (Ru–Ru) is the operative mechanism for the ground-state delocalization of the Creutz–Taube complex. The involvement of the Ru–N_p stretching vibrations is also consistent with the three-site delocalization mechanism and with the intervalence process that resembles charge transfer from an effectively anionic bridge to a pair of approximately Ru(III) sites.

Table 5 summarizes the results for the Ru–N_p and Ru–NH₃ stretches as obtained from experimental and theoretical studies to date. Experiments report vibrations mainly in the region above 700 cm⁻¹ which belong to the pyrazine and the ammonia groups and hardly distinguish the Ru–N_p and the Ru–NH₃ stretches in the region below 500 cm⁻¹.^{7,37,47,56}

**Figure 6.** Diagram indicating the nature of the vibrations: Ru–Ru symmetric stretches (Q^-), Ru–Ru translation along the bond (Q^+ ; translation t_1), translations t_2 and t_3 , and rotations r_1 and r_2 .

4. Conclusions

DFT calculations strongly suggest a homogeneous mixed valence of the ground-state Creutz–Taube complex: (1) the structure of the [II,III] is not intermediate between the [II,II] and [III,III] ones concerning the interatomic distances; (2) for the [II,II] and [II,III] structures, the difference in the Ru–N_p and Ru–N_a distances indicates strong electronic interaction between the Ru and the pyrazine ring; (3) in contrast to the [II,II] and [II,III] structures, the C–C distances in the [III,III] structure stay close to that of the free pyrazine. The electronic structures of the 4+, 5+, and 6+ compounds have been calculated with the COSMO approach. While the 4+ compound is spin-nonpolarized and the d_{yz} states are populated, the 5+ compound shows a spin-polarized electronic structure and depopulation of the d_{yz} antibonding state. The 6+ compound is also spin-polarized with depopulated antibonding d_{yz} and nonbonding $d_{x^2-y^2}$ orbitals.

When comparing the Ru–Ru related features of the vibrational spectrum for the COSMO solvated 4+, 5+, and 6+ CT models (Figure 5), it is obvious that the 5+ case is neither intermediate nor a superposition of the 4+ and 6+ cases. When $n = 5$, shorter interatomic distances have been observed as a consequence of the stronger Ru–N_p bonding. The IR spectrum of CT 5+ reflects the stronger Ru–pyrazine bonding by blue shift of the higher frequencies, when compared to $n = 4$ and 6. The Ru vibrations show the same spectral plots for the two symmetry-inequivalent Ru atoms in the tos crystal. The Ru–Ru stretch exists near two well-defined frequencies in the solid, at 145 and 285 cm⁻¹, and the translation along the bond exists at a clearly different frequency of 345 cm⁻¹. Two coupled Ru atoms in the same charge state exist, and that determines the delocalized nature of the Creutz–Taube complex.

Acknowledgment. Swiss NSF grant 200021-109358 is gratefully acknowledged.

Appendix

A vibrational mode analysis for two atoms as a part of a compound is of interest here in order to analyze their degree of coupling (Figure 6).

It is useful to start considerations with an isolated diatomic. There are six degrees of freedom which can be analyzed in normal modes. The stretch mode (Q^-) has a nonzero frequency. The five remaining normal modes, three translations and two rotations, have a frequency of zero for a free diatomic. Of particular interest here is the Q^+ translational mode, which differs just by a -1 phase factor for one of the atoms as compared to the Q^- mode.

The mode splitting between Q^- and Q^+ , $\omega_{Q^-} - \omega_{Q^+}$ is a measure for the coupling between the two atoms.

The modes of a polyatomic molecule or a crystal may be analyzed for such a coupling between two arbitrary atoms

by projecting against Q^- and Q^+ and the remaining diatomic modes. In a compound containing many atoms, each Q projected partial density of vibrational states is a small part of the total vibrational density of states. The partial vibrational density of states for each Q^\pm integrates up to one state each by our definition, while the total vibrational density of states integrates to $3N$ for a molecule of N atoms, if the contribution at frequency 0 is counted.

The projected diatomic partial vibrational density of states (pvdos) for the two Ru atoms is thus only a small part of the total vibrational density of states (vdos). In order to show the pvdos on a reasonable scale in Figures 4 and 5, the total vdos (gray) gets off scale. Especially for the full crystal model, the vdos merges into a nonresolved band.

IC8018748